Fracture as a sample preparation method for SEM analysis: implications for basalt

Irina M. GEMBITSKAYA ▪ Saint-Petersburg Mining University, Saint-Petersburg, Russia ▪ gembitckaia_im@pers.spmi.ru
Evgeniy A. VASILEV ▪ Saint-Petersburg Mining University, Saint-Petersburg, Russia ▪ vasilev_ea@pers.spmi.ru
Victoria V. KALINA ▪ Saint-Petersburg Mining University, Saint-Petersburg, Russia ▪ kvv.padi@gmail.com
Dmitry O. NAGORNOV ▪ Saint-Petersburg Mining University, Saint-Petersburg, Russia ▪ Nagornov_DO@pers.spmi.ru

Érkezett: 2025. 10. 16. ▪ Received: 16. 10. 2025. ▪ https://doi.org/10.14382/epitoanyag-jsbcm.2025.14

Abstract
Revealing of full assemblage of accessory minerals is essential for genetic modelling of any geological object. Here we discuss a method for preparing basalts for High Resolution Scanning Electron Microscopy (HR-SEM) analysis for this purpose. This method involves fracturing samples under identical conditions using an Izod pendulum. The fractures in a sample primarily propagate along grain boundaries, their interstices, and mineral inclusions, which concentrate stress; therefore, submicron mineral grains are more likely to be exposed on fractured surfaces than on polished surfaces. Here, fresh fracture surfaces were investigated in basalt samples from the Etna vents and the Tolbachik fissure zone. Crystals of minerals containing zinc, copper, nickel, sulfur, and iron were identified on fresh fracture surfaces. The morphology of submicron crystals of apatite, orthopyroxene, spinel, and copper sulfide was revealed. These crystals were not observed on polished thin sections of these specimens as they were either not brought to the surface or were chipped out. The unambiguous morphology of submicron inclusions in orthopyroxene and olivine was shown for the first time. In contrast to the thin-section surface, the fractured surface retains clear evidence of zoning in rock-forming minerals. Additionally, the distribution of accessory minerals, the morphology of crystals in pores, which is fundamentally impossible to see in thin section, and the composition of minerals within inclusions are more reliably represented on the fracture surface. Based on these findings, we suggest fracture surfaces should be more widely studied in petrogenetic research.
Keywords: HR-SEM, basalt, fracture surface, submicron inclusions, accessory minerals, Izod pendulum
Kulcsszavak: HR-SEM, bazalt, törési felület, szubmikronos zárványok, járulékos ásványok, Izod-féle ütőmű

Irina M. GEMBITSKAYA
is a Leading Researcher of Saint Petersburg Mining university, a specialist in the field of studying rocks, minerals and their artificial synthetic analogues using systems with ion, electron, and X-ray beams with various analyzers.

Evgeniy A. VASILEV
is a Leading Researcher at the Laboratory of Studying of Material Composition, Doctor of Geological and Mineralogical Sciences.

Victoria V. KALINA
is a Junior Researcher under supervision of Dr. I.M. Gembitskaya at the Laboratory of Study of Material Composition.

Dmitry O. NAGORNOV
is an Associate Professor of the Department of Geoecology The main scientific interests are focused on the development of machines and mechanisms for the extraction of renewable minerals, reducing the degree of negative anthropogenic impacts on the environment.

1. Introduction

Rock samples are commonly prepared for Scanning Electron Microscopy (SEM) analysis as thin or polished sections [1, 2]. Accurate quantitative Energy Dispersive Spectroscopy (EDS) as well as Wave Dispersive Spectroscopy (WDS) analysis can only be performed on thin or polished sections [3]. However, a thin section or polished section represents a random cut of the rock and mineral grains within it. This section only shows some of the mineral grains in the rock or the shapes of the crystals and their aggregates that the cut accidentally passed through. Additionally, accessory minerals may be absent within the polished surface and remain inaccessible for analysis. Besides, the preparation of thin sections is also commonly associated with the formation of artifacts, the most frequent of which are phase chipping, cracks, and surface contamination, caused by grinding and polishing [2, 4]. Epoxy impregnation helps reduce the number of lost phases, new cracks, introduced during sample preparation, but it has its drawbacks [5]. For example, epoxy resin fills pores and other negative relief forms, which, on the one hand, prevents the suppression of material removal and abrasive during the processing. On the other hand, resin makes it impossible to study these areas, which can provide valuable information, such as the composition of minerals condensed from volcanic gas. An alternative method of sample preparation is to create fractures. Rocks can be broken with a geologist's hammer for this reason; however, this method does not provide the opportunity to select a fixed load for a series of samples or to control the shock propagation direction. In this process, the hammer also inevitably contacts the fracture surface, causing contamination, additional fractures, and surface damage. The fresh specimen surface can be obtained using a pendulum impact tester. Many studies have investigated sample destruction due to thermal, mechanical, electrical, and physical influences [6-11]; however, these works are primarily concerned with fracture initiation and propagation. Direct fracture surface examination by High-Resolution (HR) SEM has traditionally been used for industrial materials such as ceramics, composites, and alloys [1] but not for rocks. HR-SEM has a significant role in fractography due to three features of the instrument: high resolution, large depth of field, and the ability to obtain chemical information via X-rays analysis [6]. Fracturing will occur predominantly along the weakest areas of a medium [12]; therefore, in basalt, fractures should pass through grain boundaries and pore spaces, thus preserving the 3D morphology of the rock's constituent mineral phases. Fracturing can also pass through submicron inclusions in macro crystals, which act as stress concentrators. Ideally, a fracturing method should add minimal artifacts to the sample and be reproducible. To address this, an Izod pendulum is used in this study to fracture samples under identical conditions. Using various basalt samples, we identify several types of submicron features in fracture surfaces that are fundamentally impossible to obtain on polished sections, and we also reveal the growth origin of zoning in rock-forming minerals in some cases.

1. Sample materials and analytical methods

The samples under study were selected after a preliminary investigation of basaltic lavas from the eruptions of 1941, 1975–1976, and 2012–2013 from Tolbachik (Kamchatka Peninsula, Russia) fissure zone (T) [13-15] and 2002, 2018, and 2019 from Etna (Italy) vents (E) [16-20]. The samples were previously studied in detail in both polished and thin sections [21]. In general, basalts comprise crystals of olivine, pyroxene, plagioclase, an amorphous volcanic glass phase, and accessory minerals in different proportions and contain pores [22].

The preliminary basalt samples used here were rectangular blocks of approximately 1×1×3 cm, which were determined to be free of pre-existing microcracks or other alterations based on optical microscopy inspection. During cutting the rock into blocks using a precision saw (ISOMET 4000), it was taken into account that the disturbance zone was at least 1 mm. In the proposed method, the pendulum hammer breaks the sample instantly in a selected area. Here, fractures were obtained using an Izod pendulum model Tinius Olsen IT504, which is a pendulum impact tester. The operating principle of this apparatus is based on a freely swinging pendulum impacting a sample held in a one-sided vice grip. The edge of destruction is determined by the height of the sample attachment in the vice. The machine allows one to vary the impact energy by selecting the mass of the load and its initial height, which determines the potential energy of the pendulum. Thus, this method ensures equal impact force and uniform sample destruction. The standard capacity range of the pendulum is from 2 J to 2,82 J; this can be increased to a maximum of 25 J, using different weight sets to achieve capacities of 5 J, 7,5 J, 15 J, and 25 J. The nature of the fracture in the sample material is associated with the brittleness, density, porosity and fracturing of the rock. The microstructure of a rock sample, such as the size and shape of mineral phases, the direction of crystal growth, the shape-preferred orientation of rock-forming minerals, and pre-existing microcracks, controls the process of crack initiation and propagation [23].

The fracture surfaces were coated with carbon using a Jeol JEE-4x vacuum evaporator in a dynamic tilting and rotating mode. The fractures were analyzed by SEM in secondary electron imaging (SEI) and backscattered electron imaging (BSE) modes. This study was performed using a JEOL JSM-7001F SEM equipped with a field emission cathode and an Oxford X-Max 80mm² energy dispersive spectroscopy (EDS) spectrometer. The optimal operating parameters were an accelerating voltage of 10-25 kV, a beam current of 10^{-10} A, and a working distance of 10 mm. The BSE compositional contrast mode (COMPO) was used to obtain high-resolution images illustrating the mean atomic number contrast. The fracture surface and mineral micro-nanophase morphology were studied in BSE topographic contrast (TOPO) and SEI modes. The optimal conditions for diagnosing a sample's heterogeneous chemical composition are the absence of topographic contrast, a surface orientation perpendicular to the electron probe, and a homogeneous area with a diameter of 2–3 microns [3]. A specific workflow was introduced to analyze the submicron crystals: first, the EDS spectrum was recorded at several points within a crystal. The elemental composition of the submicron grains was determined by comparing a set of characteristic lines at the points of analysis of the grain under study and in adjacent or underlying minerals. Among the measured locations, the point with minimal characteristic X-ray line intensities of the elements of the surrounding matrix was selected. As the accelerating voltage decreases, the intensity of X-ray radiation from the chemical elements of the surrounding matrix decreases, and the relative intensity of X-ray radiation from the chemical elements of the sub-micron crystals increases. The fracture surface roughness degrades the COMPO image quality and reduces the X-ray lines' intensity; however, areas with suitable contrast and X-ray intensity can be identified by changing the sample orientation. Accordingly, a five-axis target holder was used to change the samples' orientation. It should be noted that analysis cannot be performed at the bottom of deep pores because of detector shadowing, but in such a case only the pore walls closest to the fracture surface are available for study. To ensure that the phase was not introduced during sample preparation, only those grains were selected for analysis that had reliable contacts with the surrounding perfectly faceted crystals of ortho-, clinopyroxene, plagioclase or glass matrix. Overall, the method proposed in this study represents a potentially effective technique for revealing additional features in SEM analyses of hard rocks and could be more broadly applied to overcome some of the limitations of conventional polished section analyses.

2. Results

The failure mechanism of basalt at room temperature is brittle [11]. On the fracture surface mineral grains are markedly angular and have excellent crystallographic faceting.

Important features of olivine formation in basalt were reflected in the different nature of the relief of its fracture surface (*Fig. 1a*). The crystal contains a clearly distinguished core and outer zone, which can be seen in the profile of the distribution of the main chemical elements (*Fig. 1a*). The stable intensity of the silicon line confirms the absence of topographic artifacts over the profile. If the surface of the scanned region is tilted, the analyzed point can be ensured to be horizontal using a five-axis electron microscope stage. Based on the profile scanning data, a change in forsterite content (Fo = Mg/(Mg+Fe) ×100 %) is present in the outer zone. Forsterite content Fo is an important compositional indicator, used to assess the degree of evolution experienced by magmas, and calculate magma crystallization and mantle potential temperatures. The crystal core has a homogeneous composition, with a smooth, flat fracture surface. In contrast, the crystal rim exhibits a stepwise fracture pattern and the Fo% increases in this zone. The boundary between these areas is visible in the fracture topography and COMPO mode (*Fig. 1a*). However, in polished sections of such crystals, compositional heterogeneities appear more clearly (*Fig. 1b*). Thus, fracture topography can reduce the samples characterization capabilities of the COMPO mode, but at the same time it carries valuable information on fine grain properties.

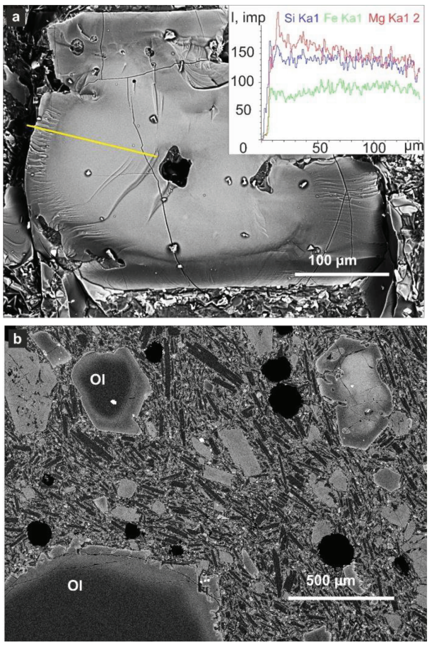

Fig. 1 Images of Tolbachik volcano basalts with large olivine crystals in BSE (COMPO) mode: a – fracture surface and the distribution of the main chemical elements in an olivine crystal (Ol: olivine). The inset shows the distribution of the characteristic line intensity of Si, Fe, Mg along the profile (yellow line) in the olivine crystal and b – polished section

1. ábra A Tolbachik vulkán bazaltjainak képei nagyméretű olivin kristályokkal, BSE (COMPO) üzemmódban: a – törési felület és a fő kémiai elemek eloszlása egy olivin kristályban (Ol: olivin). A belső kép a Si, Fe, Mg karakterisztikus vonalintenzitásának eloszlását mutatja a profil mentén (sárga vonal) az olivinkristályban; b – csiszolat

The polished surface (*Fig. 2a*) of the basalt samples sometimes exhibits some submicron-scale bright areas containing calcium and phosphorus. Based on the data obtained for this sample, the composition of the bright areas corresponds to apatite. An analysis of grains in open pores and on the fracture surface confirms the identification of this mineral as apatite. In one fracture, apatite is observed as needle-shaped hexagonal crystals (Fig. *2b, d)* with a thickness on the order of one micron or less. Submicron crystals of apatite and orthopyroxene crystallized at the olivine–plagioclase boundary are also observed on the fracture surface (*Fig. 2e*). Apatite crystals of 1–3 µm size occur as inclusions in augite and plagioclase (*Fig. 2f*) much more commonly in the fractured sample compared to its polished counterpart. The bulk morphology of the submicron phases is also clearly visible on the fracture surface, thus making the identification of these mineral species more reliable.

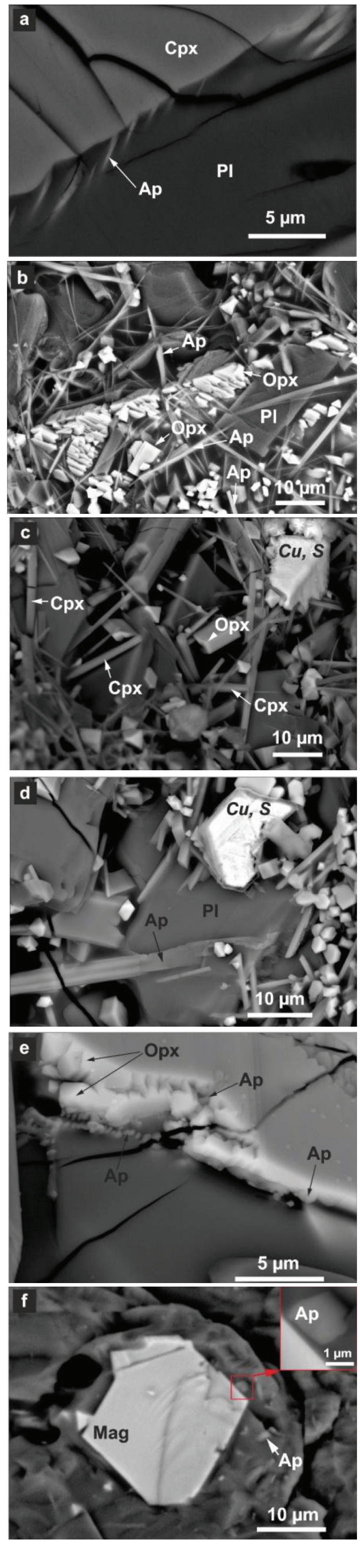

Fig. 2 Images of basalt samples in BSE (COMPO) mode: a – apatite on the polished section surface (E); b – needle-shaped apatite crystals on the fracture surface (E); c – elongated pyroxene crystals and chalcopyrite on the fracture surface (E); d – apatite and covellite on the fracture surface (E); e – apatite crystallizing on olivine on the fracture surface (T); and f – Ti-magnetite and apatite inclusions on the fracture surface in feldspar (T) (Ap: apatite; Cpx: clinopyroxene; Mag: magnetite; Opx: orthopyroxene; Pl: plagioclase)

2. ábra Bazaltminták képei BSE (COMPO) üzemmódban: a – apatit a csiszolat felszínén (E); b – tű alakú apatit kristályok a törési felszínen (E); c – megnyúlt piroxén kristályok és kalkopirit a törési felületen (E); d – apatit és kovelit a törési felületen (E); e – olivinen kristályosodó apatit a törési felszínen (T); f – Ti-magnetit és apatit zárványok a törési felületen, földpátban (T). (Ap: apatit; Cpx: klinopiroxén; Mag: magnetit; Opx: ortopiroxén; Pl: plagioklász)

The fracture also clearly reveals larger (more than 10 µm in length) grains of apatite. *Fig. 3a* shows such a crystal in clinopyroxene. *Fig. 3b* demonstrates apatite in a titanomagnetite matrix. A visible gap between the phases can be explained by differential thermal expansion of the minerals. Such inclusions are retained in the matrix only if their size is larger than the open space in the matrix. Therefore, the lack of tight contact and adhesion between the phases can have consequences during thin or polished section preparation. Inclusions can easily fall out during the cutting, grinding, or polishing stages.

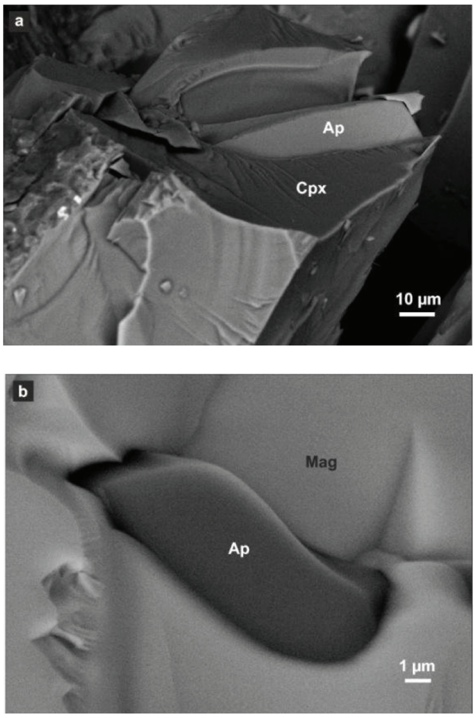

Fig. 3 Images of apatite found on the fracture surface in BSE (COMPO) mode: a – apatite in clinopyroxene (T); b – apatite in Ti-magnetite (T); (Ap: apatite; Cpx: clinopyroxene; Mag: magnetite)

3. ábra Törési felületen talált apatit képei BSE (COMPO) üzemmódban: a – apatit klinopiroxénben (T); b – apatit Ti-magnetitben (T). (Ap: apatit; Cpx: klinopiroxén; Mag: magnetit)

Many crystals of accessory minerals can be found on the fracture surface. For example, *Fig. 2f* shows well-faceted individual titanomagnetite crystals in feldspar. The morphological features of the micron and submicron pyroxene crystals and aggregates, and the oxides and sulfides of copper, zinc, iron, and nickel in lava samples from Etna and Tolbachik, are presented in *Fig. 2b-f* and *4a-f. Figure 4b* shows nickel-containing chalcopyrite in a silicate melt. In a pore space of the Etna basaltic lava sample (2002 eruption), associations of elongated pyroxene crystals with 10 µm size chalcopyrite and covellite crystals are observed (*Fig. 2c, d*). Copper also occurs as an oxide, as well-faceted crystals of cuprite (*Fig. 4c*), and as micron-sized inclusions in olivine (*Fig. 4d*) and in the silicate matrix (*Fig. 4f*), as previously reported [24]. A micron-sized phase with a dominantly copper and nickel composition was found on an elongated columnar pyroxene crystal (*Fig. 4e*). As shown, the diversity of accessory minerals is much more representative and revealed more clearly on the fracture surfaces than on the polished ones.

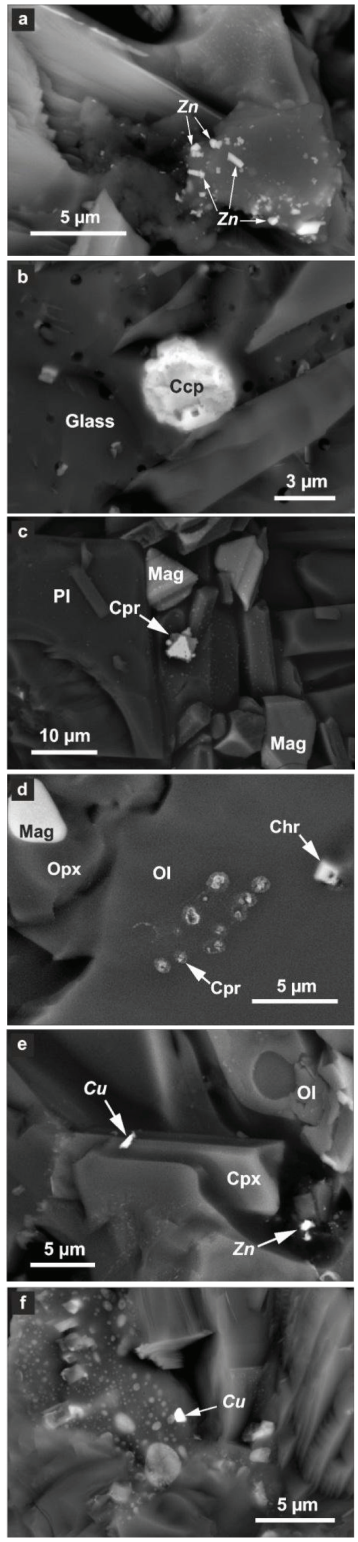

Fig. 4 Images of the fracture surface of basalts with accessory minerals in melt inclusions and pores in BSE (COMPO) mode: a – zinc in oxide form in silicate matrix (T); b – chalcopyrite with nickel admixture in a silicate melt (E); c – cuprite (T); d – cuprite in olivine (T); e – copper and nickel (left) + zinc (right) (T); f – copper in oxide form in a silicate matrix (T); (Ccp: chalcopyrite; Chr: chromite; Cpr: cuprite; Cpx: clinopyroxene; Mag: magnetite; Ol: olivine; Opx: orthopyroxene; Pl: plagioclase)

4. ábra Járulékos ásványokat tartalmazó bazalt törési felületének képei olvadékzárványokban és pórusokban, BSE (COMPO) üzemmódban: a – cink oxid formájában szilikát mátrixban (T); b – nikkel tartalmú kalkopirit szilikát olvadékban (E); c – kuprit (T); d – kuprit olivinben (T); e – réz és nikkel (balra) + cink (jobbra) (T); f – réz oxid formájában szilikát mátrixban (T). (Ccp: kalkopirit; Chr: kromit; Cpr: kuprit; Cpx: klinopiroxén; Mag: magnetit; Ol: olivin; Opx: ortopiroxén; Pl: plagioklász)

It is possible to find copper in its native form in the pore space due to the reducing environment of volcanic gases, such as sulfur dioxide (SO_2) and hydrogen sulfide (H_2S) [25]. *Fig. 5* shows a phase with a high (92-94%) copper content on plagioclase.

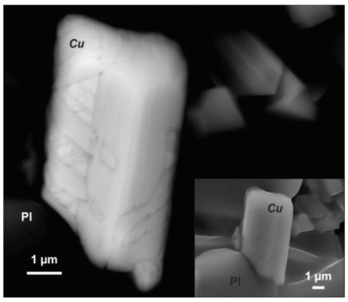

Fig. 5 Copper containing phase (Cu content according to EDS data is 92-94%) on plagioclase in BSE (COMPO) mode (T); (Pl: plagioclase). The inset shows the same area in SEI mode

5. ábra Réztartalmú fázis (a réztartalom az EDS adatok alapján 92-94%) plagioklászon, BSE (COMPO) üzemmódban (T). (Pl: plagioklász). A belső kép ugyanezt a területet mutatja SEI üzemmódban

3. Discussion

The chemical composition of the studied grains was determined after analyzing the images at different magnifications. Some zoning features are observed on the fracture surfaces of individual macro crystals. Zones with a significant change in average atomic number often exhibit differences in surface relief at the submicron scale. For example, the BSE (COMPO) images of olivine crystals from early melt crystallization exhibit an apparent direct zoning pattern represented by dark cores surrounded by bright rims, implying that the Fo% decreases towards the crystal rims [26]. Grains with direct zoning were previously studied based on compositional contrasts in polished sections [22]. Large crystals with reverse zoning were observed in basaltic lava crater facies. The COMPO mode shows a brighter crystal core surrounded by a dark rim, implying that the Fo% increases towards the crystal rim, representing reverse zoning of olivine [26]. At high resolution, the COMPO images reveal a thin zone between the core and the rim with a higher Fo% and the presence of nickel. The crystal's compositional variations were found to also be reflected in the fracture surface topography. The boundary in relief between the core and rim indicates a break in olivine crystallization; thus, the presence of a boundary in the fracture relief allows the post-growth diffusion model to be rejected for this zoning.

The morphology of the micron and submicron crystals is fully and clearly manifested on the fracture surface. This distinguishes a fracture surface from the polished surface of random cuts of crystals present in sections. The pores and inclusions are not filled with epoxy resin when fractured, thus allowing their composition to be studied at high magnification using lateral scanning. In lava samples from Etna and Tolbachik, the fracture surfaces expose numerous mineral phases containing copper, zinc, nickel, and iron in oxide and sulfide forms. Some of these mineral phases are accessory minerals in melt inclusions and pores. It is very difficult to ensure these sub-micron grains are on polished sample surfaces and even more difficult to determine their composition. Observing copper in various forms helps to determine the sample's formation mechanism [27]. Direct observation of the crystal habit of copper-bearing minerals allows sulfur deficiency in the parent lava to be estimated. We interpret that sulfur was lost from the lava as a gas during the extrusion and crystallization of the samples in this study [28; 29]. The composition of the mineral phases found in the pores is consistent with the composition of the volcanic gases recorded during the eruption [25].

A generalized diagram comparing a polished surface and a fracture is shown in *Fig. 6.* The direction of crack propagation is determined by the presence of the nearest stress concentrators in the rock. For example, grain boundaries with poor adhesion due to the contamination between the phases, which significantly reduces their real contact area [30]. Also, the preferred paths for crack propagation are intracrystalline twinning and gliding planes, inclusions in crystals and other flaws. As shown, the chemical and morphological features of the grains present in the pores and fracture surfaces provide additional information on rock-forming conditions. Studying fracture surfaces does not allow precise determination of the chemical composition of the main rock-forming minerals; however, this approach nonetheless has several important advantages. The main advantage is the conservation of all submicron-sized grains in porous and macro-grain interfaces, which can then be qualitatively analyzed. In addition, this method also allows the interpretation of submicron inclusions in macro grains.

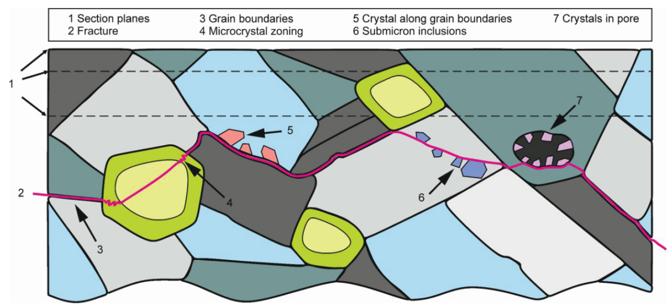

Fig. 6 Generalized diagram of the mineralogical features of the fracture propagation path through the crystallized area of a hard rock sample

6. ábra Általánosított diagram a repedés terjedési útvonalának ásványtani jellemzőiről egy kristályosodott kőzetminta területén keresztül

4. Conclusions

In this study, we reveal that investigating the fractured surface of basalt samples using HR-SEM has some crucial advantages compared to studying polished surfaces. As a direct result, sub-micron crystals of apatite, oxides and sulfides of copper, zinc, iron, and nickel were identified in lava samples from Etna and Tolbachik volcanoes. Minerals containing copper, zinc and nickel were revealed in most of the samples. Studies of fracture surfaces can also reveal microcrystal zoning, inclusions in macro crystals, and the morphology and composition of submicron crystals in pores and along grain boundaries. The results of this study show that olivine crystals exhibit changes in fracture relief at the boundary of zones with different compositions. Studying fracture surfaces allows sub-micron accessory minerals to be identified and the zoning of crystals of rock-forming minerals to be characterized in detail. Thus, the sample fracturing technique can be very useful in revealing accessory minerals in igneous and metamorphic rocks in addition to studying polished surfaces.

Data availability

The data are publicly available. Details regarding the data supporting the reported results can be found from the first author.

Competing interests

The authors declare no conflicts of interest.

References

[1] Goldstein, J.I., Newbury, D.E., Echlin, P., Joy, D.C., Lyman, C.E., Lifshin, E., Sawyer, L., & Michael, J.R. (2003). Specimen Preparation of Hard Materials: Metals, Ceramics, Rocks, Minerals, Microelectronic and Packaged Devices, Particles, and Fibers. In: Scanning Electron Microscopy and X-ray Microanalysis. *Springer, Boston, MA.* http://doi.org/10.1007/978-1-4615-0215-9_11

[2] Grundmann, G., & Scholz, H. (2015). Preparation methods in Mineralogy and Geology: The preparation of thin sections, polished sections, acetate foil prints, preparation for elutriation analysis and staining tests for the optical and electron microscopy. 26 pp.

[3] Lavrent'ev, Y.G., Karmanov, N.S., & Usova, L.V. (2015). Electron probe microanalysis of minerals: Microanalyzer or scanning electron microscope? *Russian Geology and Geophysics*, 56(8), 1154–1161. http://doi.org/10.1016/j.rgg.2015.07.006

[4] Camuti, K., & McGuire, P.T. (1999). Preparation of polished thin sections from poorly consolidated regolith and sediment materials. *Sedimentary Geology*, 128, 171–178. http://dx.doi.org/10.1016/S0037-0738(99)00073-1

[5] Kenis, P., Skurzyński, J., Jary, Z., & Kubik, R. (2020). A new methodological approach (QEMSCAN®) in the mineralogical study of Polish loess: Guidelines for further research. *Open Geosciences,* 12, 342–353. http://doi.org/10.1515/geo-2020-0138

[6] Brooks, C., & MCgill, B. (1994). The Application of Scanning Electron Microscopy to Fractography. *Materials Characterization*, 33, 195–243. http://doi.org/10.1016/1044-5803(94)90045-0

[7] Huang, D., Chang, X., Tan, Y., Fang, K., & Yin, Y. (2019). From rock microstructure to macromechanical properties based on fractal dimensions. *Advances in Mechanical Engineering,* 11(3), 1–13. http://doi.org/10.1177/1687814019836363

[8] Violay, M., Gibert, B., Mainprice, D., Evans, B., Dautria, J.M., Azais, P., & Pezard, P. (2012). An experimental study of the brittle-ductile transition of basalt at oceanic crust pressure and temperature conditions. *Journal of Geophysical Research*, 117, B03213. http://doi.org/10.1029/2011JB008884

[9] Tang Hu-dan, & Zhu Ming-li. (2020). Timely spread characteristics of micro- and meso-scale fractures based on SEM experiment. *Environmental Earth Sciences*, 79, 484. http://doi.org/10.1007/s12665-020-09224-8

[10] Zhang, Z.Z. (2015). Fractal Dimension of Fracture Surface in Rock Material after High Temperature. *Advances in Materials Science and Engineering*, 2, 1–6. http://dx.doi.org/10.1155/2015/468370

[11] Zuo, J., Wang, X., & Mao, D. (2014). SEM in-situ study on the effect of offset-notch on basalt cracking behavior under three-point bending load. *Engineering Fracture Mechanics*, 131, 504–513. http://doi.org/10.1016/j.engfracmech.2014.09.006

[12] Kjellsen, K., Monsøy, A., Isachsen, K., & Detwiler, R. (2003). Preparation of Flat-Polished Specimen for SEM-Backscattered Electron Imaging and X-Ray Microanalysis—Importance of Epoxy Impregnation. *Cement and Concrete Research*, 33, 611–616. http://doi.org/10.1016/S0008-8846(02)01029-3

[13] Churikova, T.G., Gordeychik, B.N., Edwards, B.R., Ponomareva, V.V., & Zelenin, E.A. (2015 a). The Tolbachik volcanic massif: A review of the petrology, volcanology and eruption history prior to the 2012–2013 eruption. *Journal of Volcanology and Geothermal Research*, 307, 3–21. http://doi.org/10.1016/j.jvolgeores.2015.10.016

[14] Churikova, T.G., Gordeychik, B.N., Nakamura, H., Ishizuka, O., Nishizawa, T., Haraguchi, S., Miyazaki, T., & Vaglarov, B.S. (2015 b). Petrological and geochemical evolution of the Tolbachik volcanic massif, Kamchatka, Russia. *Journal of Volcanology and Geothermal Research*, 307, 156–181. https://doi.org/10.1016/j.jvolgeores.2015.10.026

[15] Flerov, G.B., Anan'ev, V.V., & Ponomarev, G.P. (2015). The petrogenesis of rocks of the Ostryi and Ploskii volcanoes and the relationship between volcanic occurrences of basaltic and trachybasaltic magmas in the Tolbachik Dol area, Kamchatka. *Journal of Volcanology and Seismology*, 9, 162–181. http://doi.org/10.1134/S0742046315030021

[16] Clocchiatti, R., Condomines, M., Guénot, N., & Tanguy, J.C. (2004). Magma changes at Mount Etna: The 2001 and 2002–2003 eruptions. *Earth and Planetary Science Letters*, 226: 397–414. http://dx.doi.org/10.1016/j.epsl.2004.07.039

[17] Correale, A., Corsaro, R.A., Miraglia, L., Paonita, A., & Rotolo, S.G. (2024). The December 2018 eruption at Etna volcano: a geochemical study on melt and fluid inclusions. *Frontiers in Earth Science.* 11,1122132. http://doi.org/10.3389/feart.2023.1122132

[18] Lanzafame, G., Casetta, F., Giacomoni, P.P., Coltorti, M., & Ferlito, C. (2021). The Rare Trachyandesitic Lavas at Mount Etna: A Case Study to Investigate Eruptive Process and Propose a New Interpretation for Magma Genesis. *Minerals*, 11(3), 333. http://doi.org/10.3390/min11030333

[19] Métrich, N., Allard, P., Spilliaert, N., Andronico, D., & Burton, M. (2004). 2001 flank eruption of the alkali- and volatile-rich primitive basalt responsible for Mount Etna's evolution in the last three decades. *Earth and Planetary Science Letters*, 228, 1–17. http://doi.org/10.1016/j.epsl.2004.09.036

[20] Ubide, T., & Kamber, B.S. (2018). Volcanic crystals as time capsules of eruption history. *Nature Communications*, 9(1), 326. https://www.nature.com/articles/s41467-017-02244-2

[21] Gembitskaya, I., & Pharoe, B. (2023). Differentiation of Chemical Components in Basaltic Melts During Eruptions: An Example from Tolbachik–Hawaiian Fissure Zones and Etna Vent. *Proceedings of the National Academy of Sciences, India Section A*, 93, 543–552. http://doi.org/10.1007/s40010-023-00843-x

[22] Gembitskaya, I., Kotova, E.L., Abdrakhmanov, I.A., Kurovics, E., & Gömze, L.A. (2020). Insights into the applicability of the X-Ray phase quantification supported by SEM for the rock-forming silicates minerals in the basaltic lava flows. *Építőanyag: Journal of Silicate Based and Composite Materials*, 72(5), 174–177. http://doi.org/10.14382/epitoanyag-jsbcm.2020.29

[23] Přikryl, R. (2001). Some microstructural aspects of strength variation in rocks. *International Journal of Rock Mechanics and Mining Sciences*, 38, 671–682. https://doi.org/10.1016/S1365-1609(01)00031-4

[24] Lanzirotti, A., Lee, L., Head, E., Sutton, S.R., Newville, M., McCanta, M., Lerner, A.H., & Wallace, P.J. (2019). Direct measurements of copper speciation in basaltic glasses: understanding the relative roles of sulfur and oxygen in copper complexation in melts. *Geochimica et Cosmochimica Acta*, 267, 164–178. http://doi.org/10.1016/j.gca.2019.09.029

[25] Chaplygin, I.V., Lavrushin, V.Y., Dubinina, E.O., Bychkova, Y.V., Inguaggiato, S., & Yudovskaya, M.A. (2016). Geochemistry of volcanic gas at the 2012–13 New Tolbachik eruption, Kamchatka. *Journal of Volcanology and Geothermal Research*, 323, 186-193. http://dx.doi.org/10.1016/j.jvolgeores.2016.04.005

[26] Jankovics, M.É., Sági, T., Astbury, R., Petrelli, M., Kiss, B., Ubide, T., Németh, K., Ntaflos, T., & Harangi, S. (2018). Olivine major and trace element compositions coupled with spinel chemistry to unravel the magmatic systems feeding monogenetic basaltic volcanoes. *Journal of Volcanology and Geothermal Research,* 369, 203–223. http://doi.org/10.1016/j.jvolgeores.2018.11.027

[27] Sharygin, V.V., Kamenetsky, V.S., Zhitova, L.M., Belousov, A.B., & Abersteiner, A. (2018). Copper-Containing Magnesioferrite in Vesicular Trachyandesite in a Lava Tube from the 2012–2013 Eruption of the Tolbachik Volcano, Kamchatka, Russia. *Minerals,* 8, 514. http://dx.doi.org/10.3390/min8110514

[28] Cornwall, H. (1956). A summary of ideas on the origin of native copper deposits. *Economic Geology and the Bulletin of the Society of Economic Geologists,* 51, 615–631. https://doi.org/10.2113/gsecongeo.51.7.615

[29] Kamenetsky, V.S., Belousov, A., Sharygin, V.V., Zhitova, L.M., Ehrig, K., Zelenski, M.E., Chaplygin, I., Yudovskaya, M.A., Nesterenko, P.N., & Zakharov, S.M. (2019). High-temperature gold-copper extraction with chloride flux in lava tubes of Tolbachik volcano (Kamchatka). *Terra Nova,* 00, 1–7. http://dx.doi.org/10.1111/ter.12420

[30] Savanick, G.A., & Johnson, D.I. (1974). Measurements of the strength of grain boundaries in rock. *International Journal of Rock Mechanics and Mining Sciences,* 11, 173–180. https://doi.org/10.1016/0148-9062(74)90884-5

Ref.:

Gembitskaya, Irina M. – **Vasilev**, Evgeniy A. – **Kalina**, Victoria V. – **Nagornov**, Dmitry O.: *Fracture as a sample preparation method for SEM analysis: implications for basalt*

Építőanyag – Journal of Silicate Based and Composite Materials, Vol. 77, No. 4 (2025), 109–114 p.

https://doi.org/10.14382/epitoanyag-jsbcm.2025.14